INTERNATIONAL JOURNAL FOR NUMERICAL METHODS IN FLUIDS
Int. J. Numer. Meth. Fluids 2009; **59**:945–967
Published online 10 July 2008 in Wiley InterScience (www.interscience.wiley.com). DOI: 10.1002/fld.1845

Galerkin technique based on beam functions in application to the parametric instability of thermal convection in a vertical slot

N. C. Papanicolaou[1,*,†], C. I. Christov[2] and G. M. Homsy[3]

[1]*Department of Computer Science, University of Nicosia, P.O. Box 24005, 1700 Nicosia, Cyprus*
[2]*Department of Mathematics, University of Louisiana at Lafayette, Lafayette, LA 70504-1010, U.S.A.*
[3]*Department of Mechanical and Environmental Engineering, University of California at Santa Barbara, Santa Barbara, CA 93106-5070, U.S.A.*

SUMMARY

A Fourier–Galerkin spectral technique for solving coupled higher-order initial-boundary value problems is developed. Conjugated systems arising in thermoconvection that involve both equations of fourth and second spatial orders are considered. The set of so-called beam functions is used as basis together with the harmonic functions. The necessary formulas for expressing each basis system into series with respect to the other are derived.

The convergence rate of the spectral solution series is thoroughly investigated and shown to be fifth-order algebraic for both linear and nonlinear problems. Though algebraic, the fifth-order rate of convergence is fully adequate for the generic problems under consideration, which makes the new technique a useful tool in numerical approaches to convective problems.

An algorithm is created for the implementation of the method and the results are thoroughly tested and verified on different model examples. The spatial and temporal approximation of the scheme is tested. To further validate the scheme, a singular asymptotic expansion is derived for small values of the modulation frequency and amplitude and the numerical and analytic results are found to be in good agreement.

The new technique is applied to the G-jitter flow, and the Floquet stability diagrams are produced. We obtain the expected alternating isochronous and subharmonic branches and find that stable motions are always isochronous while unstable motions can be either isochronous or subharmonic. The numerical investigation also leads to novel conclusions regarding the dependence of the amplitude of the solutions on some of the governing parameters. Copyright © 2008 John Wiley & Sons, Ltd.

Received 13 February 2008; Revised 3 April 2008; Accepted 17 April 2008

KEY WORDS: spectral methods; beam functions; natural convection; singular perturbation expansion; Floquet stability; G-jitter

*Correspondence to: N. C. Papanicolaou, Department of Computer Science, University of Nicosia, P.O. Box 24005, 1700 Nicosia, Cyprus.
†E-mail: papanicolaou.n@unic.ac.cy

Contract/grant sponsor: LaSPACE Consortium under LEQSF; contract/grant number: R199524
Contract/grant sponsor: NASA; contract/grant number: NGT5-40035

1. INTRODUCTION

Fourth-order boundary value problems in continuum mechanics arise in both elasticity and viscous fluid dynamics. The simplified 1D models are, respectively, the beam equation and the equation for the stream function of the pressure-driven parallel flow between two plates (plane Poiseuille flow). A method developed for one of these fields can easily be applied to the other. The numerical treatment of multi-dimensional problems of mechanics of continua can be much more complicated because of the fact that the models are not evolutionary systems (Cauchy–Kovalevskaya type) and that the boundary value problems are of higher order. Both these difficulties can be alleviated if a suitable spectral technique is developed in the sense that the basis set of functions satisfies all of the boundary conditions.

Although the spectral approach to single-equation models is more or less clear, this is not the case when the main fourth-order equation is coupled to an equation for temperature or for another scalar variable. The boundary value problem for the additional function can differ from the one for the main unknown function. For the sake of definiteness, we will focus our attention on parallel flow created by thermal convection in a vertical slot.

There is a compelling need to develop fast spectral methods that will lead to more efficient algorithms. Such algorithms would allow a rapid interrogation of the parameter space in order to discover and understand mechanisms of flow and instability. The performance of a spectral method depends heavily on the type of the basis system. Naturally, a basis system of functions, which does not satisfy all the boundary conditions, such as Fourier functions, would exhibit very poor convergence (second-order algebraic with the number of terms). An elucidating discussion on the performance of different sets of functions can be found in the encyclopedic book of Boyd [1]. The algebraic convergence is limited by the presence of boundary conditions. If the system of functions satisfies four boundary conditions, the asymptotic order of convergence becomes fourth-order algebraic. This means that a mere number of 50 terms would bring accuracy of 10^{-7}, which roughly corresponds to taking 10 000 points in a second-order difference scheme in the interval $[-1, 1]$. A system of orthonormal functions on the interval $[-1, 1]$ that satisfies four boundary conditions was introduced by Lord Rayleigh and is known as the *beam functions*, see [2].

The application of the beam-Galerkin method to plane Poiseuille flow is at present well developed, see [3, 4]. We go a step further here and consider the generic boundary value problem for convective flows of viscous liquids. Because of the complexity of the convection problems, even the geometrically simplified situations are intensively researched in order to identify the physical mechanisms. The same mechanisms are often operative in more complicated situations and the information gathered from the simple geometries is very useful. Even for the simplest geometries with plane-parallel flows, the mathematical models are represented by higher-order boundary value problems in one and two dimensions and exact analytical solutions are not available. The requirements for accuracy and stability of the numerical schemes are very demanding because of the bifurcation character of the flows. At the same time, the parametric space of physical interest and significance are large, with typically four to five dimensionless parameters involved. The Rayleigh number and modulation frequency can take on very high values, signaling the occurrence of boundary or internal layers of steep profiles of the field variables, which makes the development of effective numerical approaches a must.

In the present study, the beam-Galerkin spectral expansion is verified for internal consistence and shown to have fifth-order algebraic rate of convergence (some preliminary accounts about the

DOI: 10.1002/fld

technique can be found in [5–7]). In order to have an independent verification of the performance of the algorithm, we find a perturbation approximate solution of boundary-layer type for both the temperature and stream function. Separate expressions are found for the boundary and outer layer and then these are matched, yielding uniform approximate solutions valid for the whole interval $[-1, 1]$. These results verify the solutions obtained using our numerical technique.

2. THERMAL CONVECTION IN A VERTICAL SLOT

Consider the 2D flow in a vertical slot with a linear vertical temperature gradient and differentially heated walls, when the flow is subjected to gravity modulations. The problem is well described in the literature (refer [8, 9] and Figure 1 for a definition sketch), and the notation we use is standard:

$$x=\frac{x^*}{L}-1, \quad y=\frac{y^*}{L}, \quad \omega=\omega^*\frac{L^2}{\kappa}, \quad t=t^*\omega^*, \quad \psi=\frac{\psi^*}{\nu}, \quad \theta=\frac{T^*}{\delta T}+x-\tau_B y$$

where ν is the kinematic viscosity, κ the thermal diffusivity, $2L$ the width of the slot, δT the horizontal temperature difference, and τ_B the dimensionless vertical gradient. The asterisk denotes dimensional variables, while the same notation without an asterisk stands for the respective dimensionless quantity. The combined influence of the horizontal and vertical stratification makes the phenomenology of this flow very rich. Note that the field $\theta(x, y, t)$ is the departure from the linear vertical and horizontal stratification. Hence, one can seek solutions that are periodic in the vertical direction.

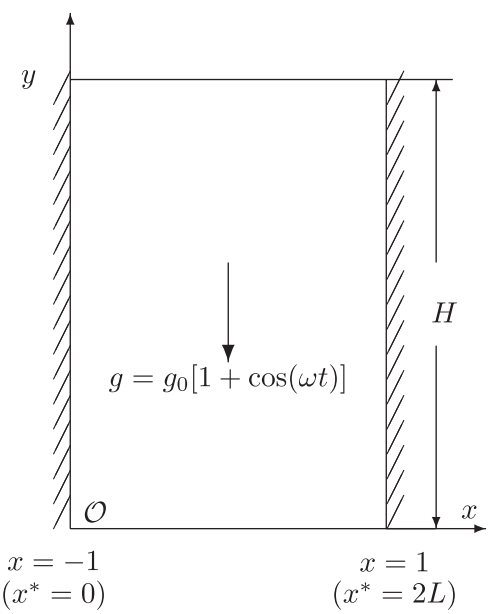

Figure 1. Flow geometry.

DOI: 10.1002/fld

The dimensionless boundary value problem under consideration reads

$$\frac{1}{Pr}\left(\omega\frac{\partial\Delta\psi}{\partial t}+\frac{\partial\psi}{\partial y}\frac{\partial\Delta\psi}{\partial x}-\frac{\partial\psi}{\partial x}\frac{\partial\Delta\psi}{\partial y}\right)=-Ra\left(\frac{\partial\theta}{\partial x}-1\right)[1+\varepsilon\cos(t)]+\Delta^2\psi \tag{1}$$

$$\omega\frac{\partial\theta}{\partial t}+\left(\frac{\partial\psi}{\partial y}\frac{\partial\theta}{\partial x}-\frac{\partial\psi}{\partial x}\frac{\partial\theta}{\partial y}\right)=\frac{\partial\psi}{\partial y}+\tau_B\frac{\partial\psi}{\partial x}+\Delta\theta \tag{2}$$

with boundary conditions

$$\psi=\frac{\partial\psi}{\partial x}=\theta=0 \quad \text{for } x=\pm1 \tag{3}$$

and periodic conditions in vertical direction

$$\begin{aligned}
\psi(x,0,t)&=\psi(x,H,t), \quad \psi_y(x,0,t)=\psi_y(x,H,t)\\
\psi_{yy}(x,0,t)&=\psi_{yy}(x,H,t), \quad \psi_{yyy}(x,0,t)=\psi_{yyy}(x,H,t)\\
\theta(x,0,t)&=\theta(x,H,t), \quad \theta_y(x,0,t)=\theta_y(x,H,t)
\end{aligned} \tag{4}$$

where $H=H^*/L=2\pi/\alpha$ is the dimensionless height of the vertical box: equivalently, α is the dimensionless vertical wave number of the periodic solutions.

The Rayleigh number Ra, the Prandtl number Pr, and stratification parameter γ are defined as

$$Ra=\frac{\beta g_0\delta T L^3}{\nu\kappa}, \quad Pr=\frac{\nu}{\kappa}, \quad 4\gamma^4=\tau_B Ra$$

where β is the coefficient of thermal expansion of the liquid, g_0 the mean gravity, ε the dimensionless amplitude of gravity modulations, ω the dimensionless frequency, and τ_B the dimensionless vertical temperature gradient. Using a difference approximation and an operator splitting, the 2D flow was investigated numerically in [10]. We focus our attention on the 1D case for the purposes of developing the new numerical technique.

As has been shown by Farooq and Homsy [11], the problem also admits a plane-parallel solution of the form $\Psi(x,t)$, $\Theta(x,t)$ for which the governing system reduces to the following:

$$\frac{1}{Pr}\frac{\partial^3\Psi}{\partial t\partial x^2}=-Ra\left[-1+\frac{\partial\Theta}{\partial x}\right][1+\varepsilon\cos(\omega t)]+\frac{\partial^4\Psi}{\partial x^4} \tag{5}$$

$$\frac{\partial\Theta}{\partial t}=\tau_B\frac{\partial\Psi}{\partial x}+\frac{\partial^2\Theta}{\partial x^2} \tag{6}$$

with the same boundary conditions given in (3).

The 1D flow was first treated in [9] where different regimes of flow were studied. The parametric bifurcation of the 1D solutions was studied in detail in [10] by means of a fully implicit difference scheme. A related 1D problem was investigated in [12]. This flow can therefore be used as a testing ground for the new technique developed here.

The main problem with using FD or FEM technique for investigating a bifurcation is that the process of solution branching is very sensitive to the order of approximation of the scheme. When

DOI: 10.1002/fld

there is more than one nontrivial solution, the small impurities of the approximation affect the way the algorithm chooses one or the other branching solution. It is imperative to have an alternative technique to solve the problem in order to verify the findings.

A way out of the above-described difficulties is to use spectral decomposition with respect to complete orthonormal (CON) system of functions of x-coordinate. The performance of a spectral method depends heavily on the type of the basis system of functions. The scope of this paper is to implement these ideas for the 1D in space time-dependent problem (3), (5), (6).

3. THE SPECTRAL TECHNIQUE

The expansion in the x direction is nontrivial because of the higher-order boundary value problem for the stream function. The appropriate CON system was introduced by Lord Rayleigh for the problem of vibration of elastic beams. For the specific boundary conditions arising in viscous liquid dynamics, the system and some discussion about its completeness can be found in [13]. The product formulas as well as the expansion formulas for the derivatives of different orders were derived by Christov [4]. The product formula is essential for a Galerkin-type approximation of nonlinear problems. Since the problem considered in the present paper is linear, we present the product formulas in Appendix B and refer the reader to [14]. In this section, we treat the matter systematically in order to develop a reliable and generally useful Galerkin spectral technique.

Consider the Sturm–Liouville problem

$$\frac{\mathrm{d}^4 u}{\mathrm{d}x^4} = \lambda^4 u, \quad u = \frac{\mathrm{d}u}{\mathrm{d}x} = 0 \quad \text{for } x = \pm 1 \tag{7}$$

The nontrivial solutions (eigenfunctions) of this problem are given by

$$s_m = \frac{1}{\sqrt{2}} \left[\frac{\sinh \lambda_m x}{\sinh \lambda_m} - \frac{\sin \lambda_m x}{\sin \lambda_m} \right], \quad \coth \lambda_m - \cot \lambda_m = 0 \tag{8}$$

$$c_m = \frac{1}{\sqrt{2}} \left[\frac{\cosh \kappa_m x}{\cosh \kappa_m} - \frac{\cos \kappa_m x}{\cos \kappa_m} \right], \quad \tanh \kappa_m + \tan \kappa_m = 0 \tag{9}$$

Because of the original motivation that led to their development, these functions are sometimes called beam functions. A major step in the advancement of the application of the beam functions to fluid-dynamics problems was made by Poots [3]. The magnitudes of the different eigenvalues can be found in most of the above cited works from the literature.

Chandrasekhar [13] derived their counterparts for problems with cylindrical symmetry. For applications to stability problems, see also [15, 16].

The different derivatives can be expressed in series with respect to the system as follows:

$$c_n' = \sum_{m=1}^{\infty} a_{nm} s_m, \quad s_n' = \sum_{m=1}^{\infty} \bar{a}_{nm} c_m, \quad a_{nm} = -\bar{a}_{mn} = \frac{4\kappa_n^2 \lambda_m^2}{\kappa_n^4 - \lambda_m^4} \tag{10}$$

$$c_n''' = \sum_{m=1}^{\infty} d_{nm} s_m, \quad s_n''' = \sum_{m=1}^{\infty} \bar{d}_{nm} c_m, \quad d_{nm} = -\bar{d}_{mn} = \frac{4\kappa_n^3 \lambda_m^3}{-\kappa_n^4 + \lambda_m^4} \tanh \kappa_n \coth \lambda_m \tag{11}$$

DOI: 10.1002/fld

$$c_n'' = \sum_{m=1}^{\infty} \beta_{nm} c_m, \quad \beta_{nm} = \begin{cases} \dfrac{4\kappa_n^2 \kappa_m^2}{\kappa_m^4 - \kappa_n^4} (\kappa_m \tanh \kappa_m - \kappa_n \tanh \kappa_n), & m \neq n \\ \kappa_n \tanh \kappa_n - (\kappa_n \tanh \kappa_n)^2, & m = n \end{cases} \tag{12}$$

$$s_n'' = \sum_{m=1}^{\infty} \bar{\beta}_{nm} s_m, \quad \bar{\beta}_{nm} = \begin{cases} \dfrac{4\lambda_n^2 \lambda_m^2}{\lambda_n^4 - \lambda_m^4} (\lambda_n \coth \lambda_n - \lambda_m \coth \lambda_m), & m \neq n \\ \lambda_n \coth \lambda_n - (\lambda_n \coth \lambda_n)^2, & m = n \end{cases} \tag{13}$$

In order to be able to treat the inhomogeneous terms, one needs the expansions of different functions in beam-Galerkin series. For the purposes of the present study, it is enough to have the expansions of unity and the trigonometric functions.

For the expansion of unity into a c_m series, we have

$$1 = \sum_{k=1}^{\infty} h_k c_k(x), \quad h_k = \int_{-1}^{1} c_k(x)\, \mathrm{d}x = \frac{2\sqrt{2} \tanh \kappa_k}{\kappa_k} \tag{14}$$

The convergence of the last expansion is algebraic of first order. This is due to the fact that unity does not satisfy the boundary conditions for the beam functions and as a result a strong Gibbs effect is observed near the boundaries. Yet, as it will be shown later in the text, the overall rate of convergence of the method is fifth-order algebraic, because in the left-hand side of the problems under consideration, the fourth power of the respective eigenvalue appears as a multiplier.

For the convective flow under consideration, the boundary value problem for temperature function is of second order, which means that the system of beam functions is not suitable for expanding the temperature field. It is clear that the system best suited to the task is the trigonometric *sines* and *cosines*. Hence, we need to develop expressions for expanding the beam functions into trigonometric functions and *vice versa* (see [5, 6]):

$$\sin l\pi x = \sum_{k=1}^{\infty} \sigma_{lk} s_k(x), \quad \sigma_{lk} = \frac{2\sqrt{2} l\pi (\lambda_k)^2 (-1)^l}{l^4\pi^4 - \lambda_k^4} \tag{15a}$$

$$\cos l\pi x = \sum_{k=1}^{\infty} \chi_{lk} c_k(x), \quad \chi_{lk} = \frac{2\sqrt{2} \kappa_k^3 (-1)^{l+1} \tanh \kappa_k}{l^4\pi^4 - \kappa_k^4} \tag{15b}$$

$$c_n(x) = \sum_{l=1}^{\infty} \hat{\chi}_{nl} \cos l\pi x, \quad \hat{\chi}_{nl} = \frac{2\sqrt{2} \kappa_n^3 (-1)^{l+1} \tanh \kappa_n}{l^4\pi^4 - \kappa_n^4} \tag{15c}$$

$$s_n(x) = \sum_{l=1}^{\infty} \hat{\sigma}_{nl} \sin l\pi x, \quad \hat{\sigma}_{nl} = \frac{2\sqrt{2} l\pi (\lambda_n)^2 (-1)^l}{l^4\pi^4 - \lambda_n^4} \tag{15d}$$

Once again we point out that the convergence when expanding $\cos(l\pi x)$ in a series in c_k is first order, i.e. $O(k^{-1})$ (see (15b)) due to the fact that it does not satisfy both boundary conditions for the beam functions. It satisfies the condition on the derivatives but fails to satisfy the conditions on the function itself. Clearly, the situation with $\sin(l\pi x)$ is slightly better (it satisfies two of the boundary conditions), and as a result, the rate of convergence is of second order, i.e. $O(k^{-2})$

DOI: 10.1002/fld

(see (15a)). Thus, the disagreement is more subtle since only the conditions on the first derivative are not satisfied. The situation with the expansions of beam function s_k and c_k in Fourier series is reversed. The order of convergence for c_k is $O(l^{-4})$ (see (15c)), and for s_k it is $O(l^{-3})$ (see (15d)). As it will be shown in what follows, this property is of crucial importance for the overall rate of convergence.

In addition to the preceding considerations, following the method demonstrated by Boyd [1], we can prove that the convergence rate of our solutions is fifth-order algebraic. First, we show the following lemma relative to the boundary value problem (BVP) (5), (6), (3):

Lemma 3.1
$\Theta(x,\cdot), \Psi(x,\cdot) \in \mathscr{C}^5([-1,1])$.

Proof
Since $\Psi \in \mathscr{C}^4([-1,1])$, then $\Psi_x \in \mathscr{C}^3([-1,1])$. As a result we get from (6) that $\Theta_{xx} \in \mathscr{C}^3([-1,1])$, which gives $\Theta \in \mathscr{C}^5([-1,1])$. In turn, this implies $\Theta_x \in \mathscr{C}^4([-1,1])$ and by (5) we have the result. □

Now we are ready to prove the following theorem:

Theorem 3.1
Let $\Psi(x,\cdot), \Theta(x,\cdot) \in \mathscr{C}^5([-1,1])$. Then, the convergence rate of both the spectral series for the solution of problem (3), (5), (6) is fifth-order algebraic.

Proof
The spectral series for the stream function and temperature are given by

$$\Psi(x,t) = \sum_{k=1}^{K} p_k c_k(x), \quad \Theta(x,t) = \sum_{k=1}^{K} d_k \sin(k\pi x) \tag{16}$$

respectively. First we prove the theorem for Ψ. By definition,

$$p_k = \int_{-1}^{1} c_k(x)\Psi(x,\cdot)\,\mathrm{d}x \tag{17}$$

After successive integrations by parts, acknowledging the value of $c_k(x)$ at the boundary and the characteristic equation $\tanh\kappa_k + \tan\kappa_k = 0$ and using (3), we get

$$p_k = \left[\frac{\Psi_{xxxx}}{\sqrt{2}\kappa_k^5}\left(\frac{\sinh\kappa_k x}{\cosh\kappa_k} - \frac{\sin\kappa_k x}{\cos\kappa_k}\right)\right]_{x=-1}^{x=1} - \frac{1}{\sqrt{2}\kappa_k^5}\int_{-1}^{1}\left(\frac{\sinh\kappa_k x}{\cosh\kappa_k} - \frac{\sin\kappa_k x}{\cos\kappa_k}\right)\Psi_{xxxxx}\,\mathrm{d}x \tag{18}$$

Because of the lack of differentiability of Ψ beyond the fifth order, we cannot continue the process of integration by parts any further.

Again, following successive integrations by parts, acknowledging the value of $\sin(k\pi x)$ at the boundary, and using (3) and the fact that $\Theta_{xx}(\pm 1) = 0$ because of (3), (6) we get

$$d_k \overset{\text{def}}{=} \int_{-1}^{1} \sin(k\pi x)\Theta(x,\cdot)\,\mathrm{d}x = \left[-\frac{\Theta_{xxxx}}{k^5\pi^5}\cos k\pi x\right]_{x=-1}^{x=1} + \frac{1}{k^5\pi^5}\int_{-1}^{1}\Theta_{xxxxx}\cos k\pi x\,\mathrm{d}x \tag{19}$$

DOI: 10.1002/fld

Note that in the proof for Θ, the main reason for stopping after the fifth integration by parts is that the first term in (19) is nonzero. □

4. VALIDATIONS OF THE TECHNIQUE

In order to assess the approximation, convergence rate and truncation error, it is enough to consider a model ODE, which contains all of the different terms of the time-dependent system. A simplified first step is to consider just one ODE of fourth order. To this end we consider three boundary value problems.

We present the numerical tests and verifications of the Galerkin technique using as featuring examples the three boundary value problems.

4.1. A linear model problem

Consider a BVP containing both fourth- and second-order derivatives:

$$\frac{\mathrm{d}^4u}{\mathrm{d}x^4}+2\frac{\mathrm{d}^2u}{\mathrm{d}x^2}+u=1, \quad u(-1)=u(1)=0, \quad u'(-1)=u'(1)=0 \tag{20}$$

which possesses an analytical solution:

$$u(x)=1-\frac{2\cos x[\cos 1+\sin 1]-2x\sin 1\sin x}{2+\sin 2} \tag{21}$$

We solve (20) numerically using the developed here beam-Galerkin expansion with respect to the CON system of functions $c_n(x)$, $s_n(x)$. Because of the nature of the boundary conditions, we can constrain ourselves to the subset of even functions c_n (a fact also verified by the analytic solution) and expand the sought function into series with respect to $c_n(x)$:

$$u(x)=\sum_1^N b_i c_i(x) \tag{22}$$

We introduce this series into Equation (20), multiply all terms by the test functions $c_j(x)$, $j=1,\ldots,N$, and integrate with respect to x over $[-1,1]$. Using orthonormality of the beam functions and the formulas compiled in Section 3, we obtain the following linear algebraic system of N equations with N unknowns for the coefficients b_i:

$$\sum_{j=1}^{N}[(1+\kappa_i^4)\delta_{ij}+2\beta_{ij}]b_j=\frac{2\sqrt{2}\tanh\kappa_i}{\kappa_i} \quad \text{for } i=1,\ldots,N \tag{23}$$

with β_{ij} defined in (12), Section 3.

The algebraic system (23) for the coefficients is solved using the LAPACK routine DGESV. We found that the coefficients b_i decay with the number of the terms i as i^{-5}, which is clearly seen in Figure 2(a) where the values of the computed spectral coefficients are presented. As is to be expected for a series with fifth-order algebraic convergence, the ratio of b_{100} to b_1 is of order $O(10^{-10})$, which confirms the fifth-order algebraic convergence.

DOI: 10.1002/fld

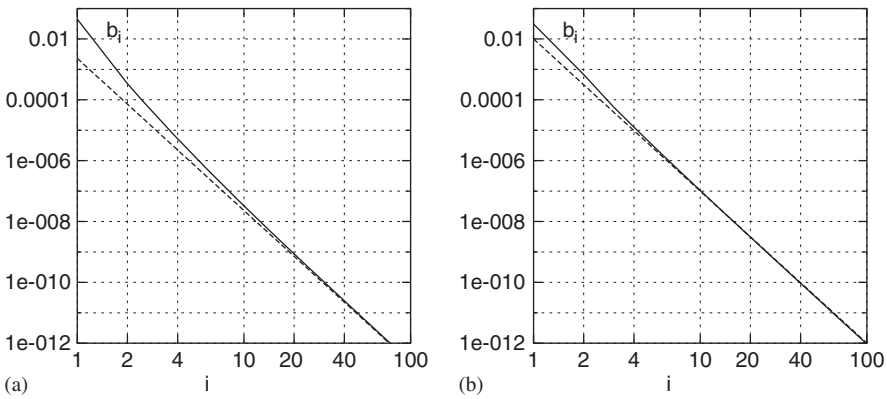

Figure 2. Convergence of the beam-Galerkin series for the model: solid line, computed b_i; dashed line, the best fit curve. (a) Equation (20) with $b_i = 0.0023i^{-5}$ and (b) Equation (24) with $b_i = 0.01i^{-5}$.

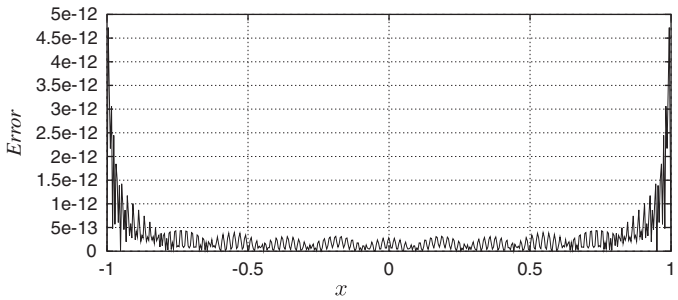

Figure 3. The absolute value of the difference between the exact analytic and spectral ($N = 100$) solutions of the linear model problem.

The pointwise truncation error is presented in Figure 3.

4.2. A nonlinear model problem

A nonlinear version of the problem from Section 4.1 is as follows:

$$\frac{\mathrm{d}^4 u}{\mathrm{d}x^4} + 2\frac{\mathrm{d}^2 u}{\mathrm{d}x^2} + u = 1 - 100u^2(x) \tag{24}$$

$$u(-1) = u(1) = 0, \quad u'(-1) = u'(1) = 0 \tag{25}$$

where the large coefficient 100 multiplying the nonlinear term is selected for the sake of making the nonlinearity more significant. Although the bifurcation problem of the present study is linear, we present the validations of the nonlinear terms for completeness. For more details we refer to [14].

DOI: 10.1002/fld

Following the same procedure as before, we find that the nonlinear problem (24) results in the following nonlinear algebraic system of N equations with N unknowns:

$$(1+\kappa_i^4)b_i + 2\sum_{j=1}^{N} b_j\beta_{ij} = \frac{2\sqrt{2}\tanh\kappa_i}{\kappa_i} - 100\sum_{m=1}^{N}\sum_{n=1}^{N} b_m b_n h_i^{mn} \quad \text{for } i=1,\ldots,N \tag{26}$$

where h_i^{mn} is defined in formula (B1). We solve the latter with semi-implicit method and iterations. The results about the convergence of the spectral solution are shown in Figure 2(b). The convergence is once again fifth-order algebraic.

4.3. A coupled system

In order to test the performance of the formulas for cross-expansion between the beam and harmonic functions, we consider the following higher-order coupled stationary BVP, which retains all of the important spatial derivatives from the fully fledged unsteady thermal convection problem:

$$\frac{\mathrm{d}^4\Psi}{\mathrm{d}x^4} = -Ra\left[-1+\frac{\mathrm{d}\Theta}{\mathrm{d}x}\right] + \frac{1}{Pr}\frac{\mathrm{d}^2\Psi}{\mathrm{d}x^2} \tag{27}$$

$$\Theta - \frac{\mathrm{d}\Psi}{\mathrm{d}x} = \frac{\mathrm{d}^2\Theta}{\mathrm{d}x^2}, \quad \Psi=\Psi_x=\Theta=0 \quad \text{for } x=\pm 1 \tag{28}$$

Because of the obvious symmetry of the boundary value problem under consideration, we can seek a solution in which the stream function is an even and the temperature is an odd function. Acknowledging the symmetry of the problem, we develop the sought function into the series

$$\Psi(x,t) = \sum_{k=1}^{K} p_k c_k(x), \quad \Theta(x,t) = \sum_{k=1}^{K} d_k \sin(k\pi x) \tag{29}$$

We introduce these expansions into (28) and use the formulas of Section 3 to convert all the terms of the first of the coupled equations into even beam functions and all terms of the second equation into sines. Then we multiply the first of the equations by $c_n(x)$, $n=1,\ldots,N$, and the second by $\sin(m\pi x)$, $m=1,\ldots,N$, and integrate over $[-1,1]$. Taking advantage of the orthonormality of the beam and trigonometric functions, employing derivative formula (12) and cross-expansion formulas (15b), (15d), we derive an algebraic system for the coefficients d_k and p_k

$$-\kappa_i^4 p_i + \frac{1}{Pr}\sum_{j=1}^{N} p_j\beta_{ij} = -Ra\left[\sum_{m=1}^{N} d_m \frac{m\pi 2\sqrt{2}(-1)^{m+1}\kappa_i^3\tanh\kappa_i}{m^4\pi^4-\kappa_i^4} - \frac{2\sqrt{2}\tanh\kappa_i}{\kappa_i}\right] \tag{30}$$

$$(1+l^2\pi^2)d_l = \tau_B\sum_{j=1}^{N}\sum_{m=1}^{N} p_j \frac{8\sqrt{2}\kappa_j^2\lambda_m^4 l\pi(-1)^l}{(\kappa_j^4-\lambda_m^4)(l^4\pi^4-\lambda_m^4)} \tag{31}$$

for $=1,\ldots,N$. The results for the coefficients p_i and d_i are presented in Figure 4.

The fifth-order convergence rate is once again observed for this more complicated case. It means that the number of terms $N=100$ gives a very high precision 10^{-10}. Even $N=30$ is adequate enough, since it gives precision 10^{-8}. This demonstrates the advantage of the spectral technique over the finite-difference scheme with reasonable resolution on a uniform grid. Only a grid of size 10000 can come close to the accuracy of the beam spectral method with $N=30$ terms.

DOI: 10.1002/fld

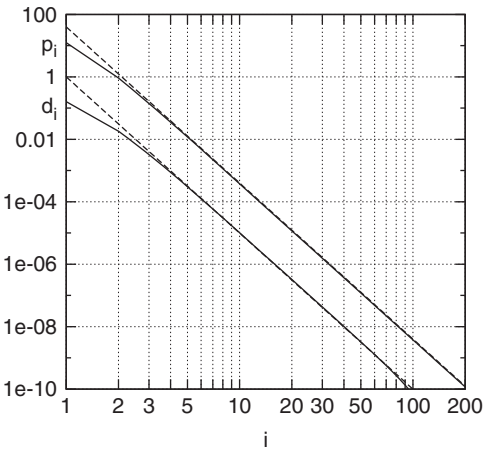

Figure 4. The rate of convergence for the coupled system for $Ra=1000$, $Pr=0.73$, and $\tau_B=0.16$. Upper solid line: p_i. Accompanying dashed line: the best fit $p_i=40i^{-5}$. Lower solid line: Fourier–Galerkin coefficients of temperature d_i. Accompanying dashed line: the best fit $d_i=i^{-5}$.

5. THE UNSTEADY THERMOCONVECTIVE FLOW

5.1. The Galerkin spectral method

The spatial approximation, convergence rate, and truncation error were discussed in Section 4 where three model ODE problems were solved: a fourth-order linear BVP, a nonlinear fourth-order BVP, and a coupled problem containing all of the different terms of the time-dependent system. It was found that with only 30 terms in the spectral series the error was of $O(10^{-8})$ and with 100 terms the error was reduced to a very low level of $O(10^{-10})$.

In this section we outline the algorithm for the unsteady thermoconvective flow (the *jitter* flow). For the sake of convenience, we introduce the following notations:

$$b_{kl}=\sum_{m=1}^{N}\hat{\sigma}_{ml}a_{km} \tag{32}$$

where a_{km} and $\hat{\sigma}_{ml}$ are from (10) and (15d), respectively.

For the time stepping we use a staggered second-order Crank–Nicolson-type scheme for the time stepping, i.e.

$$\sum_{j=1}^{N}\beta_{ij}\frac{p_i^{n+1}-p_i^n}{\tau Pr}=-Ra\left[\sum_{l=1}^{N}\pi l\chi_{li}d_l^{n+1/2}-\frac{2\sqrt{2}\tanh\kappa_i}{\kappa_i}\right][1+\varepsilon\cos(n\omega\tau)]+\kappa_i^4\frac{p_i^{n+1}+p_i^n}{2} \tag{33}$$

$$\frac{d_l^{n+3/2}-d_l^{n+1/2}}{\tau}=\tau_B\sum_{j=1}^{N}b_{jl}p_j^{n+1}-l^2\pi^2\frac{d_l^{n+3/2}+d_l^{n+1/2}}{2} \tag{34}$$

where $\{p_i\}_{i=1}^N$, $\{d_l\}_{l=1}^N$ are the spectral coefficients of the stream function and temperature, respectively, and the superscripts denote the time stage.

DOI: 10.1002/fld

The stability of Crank–Nicolson schemes is well documented; therefore, we expect scheme (33), (34) to exhibit a stable behavior in time. Note that the matrix $B=\{Pr^{-1}\beta_{ij}-\tau\kappa_i^4\delta_{ij}\}$ that multiplies the vector $\{p_i^{(n+1)}\}$ is negative definite for reasonable values of the time step τ (order $O(10^{-2})$ or greater) and the norm of its inverse is $\|B^{-1}\|<1$. This is because all the eigenvalues of B are negative and increase in magnitude with the size of the matrix $N\times N$. Also, the matrix $D=\{(1/\tau+l^2\pi^2/2)\delta_{ll}\}$ that multiplies the vector $\{d_l^{(n+3/2)}\}$ is positive definite with eigenvalues that increase proportionally to N^2. Thus, $\|D^{-1}\|<1$.

The inversion of the diagonal matrix in Equation (34) is trivial. The inversion of the matrix in Equation (33) can be performed just once in the beginning of the algorithm and then the inverse can be used during the time stepping to multiply the r.h.s. of (33). This means that the computational cost of the above implicit scheme is equal to the cost of an explicit scheme, which makes it highly efficient. The inversion of the matrix in Equation (33) is performed with the aid of LAPACK routine DGETRI for symmetric full matrices.

We tested the algorithm for the case $\varepsilon=0$ when a steady-state solution is reached and verified that it is of fifth-order algebraic convergence. This is due to the fact that in the limit $t\to\infty$, the term containing the matrix b_{ij} with the off-diagonal terms disappear and the rest of the terms have already been shown to yield fifth-order accuracy.

Apart from proving its internal consistence, rate of approximation, and convergence, the best verification of a numerical method is to compare its prediction with an analytical solution in some limiting cases. As has been noted previously, problem (3), (5), (6) does not possess an exact analytic solution. However, for $\omega\sim O(1)$, $\varepsilon\leqslant 1$ it can be treated by a perturbation technique and approximate analytic solutions can be found for this range of parameters. It has been pointed out in [10] that the magnitude of the parameter of vertical stratification γ ($4\gamma^4=\tau_\beta Ra$) plays a most important role in defining the profiles of the velocity and temperature. For the sake of convenience we incorporate the large parameter Ra in the scalings and rewrite our coupled system of equations in terms of $\psi=\Psi/Ra$.

It is possible to construct a matched singular asymptotic expansion with respect to the small parameter $\delta=1/\gamma$, when $\gamma\gg 1$. The details of this asymptotic solutions can be found in [17]. Here we present the solution within the order $O(\delta)$:

$$\theta^u=x+\exp\frac{-a(x+1)}{\delta}\cos\frac{a(x+1)}{\delta}-\exp\frac{a(x-1)}{\delta}\cos\frac{-a(x-1)}{\delta}+O(\delta) \tag{35}$$

$$\psi^u=\frac{1}{4}a\delta^3\left\{\exp\frac{-a(x+1)}{\delta}\cos\frac{a(x+1)}{\delta}+\exp\frac{-a(x+1)}{\delta}\sin\frac{a(x+1)}{\delta}\right.$$
$$\left.+\exp\frac{a(x-1)}{\delta}\cos\frac{a(1-x)}{\delta}+\exp\frac{a(x-1)}{\delta}\sin\frac{a(1-x)}{\delta}-1\right\}+O(\delta) \tag{36}$$

where $a(t)=[1+\varepsilon\cos(\omega t)]^{1/4}$.

We have chosen the case $\gamma=12$, $\omega=3$, $\varepsilon=1$, which is near the border of the parameter range for which our perturbation method is valid. This is a good choice for our purposes since the numerical method fails for vanishingly small values of the modulation frequency. The reason is that for such small values of ω a very fine time resolution is required (e.g. 1000 time steps per period) making the algorithm inefficient. Also, for $\varepsilon>1$ (35) and (36) become invalid since $a(t)=(1+\varepsilon\cos(\omega t))^{1/4}$ may become a complex number, thus changing the form of the solution. The snapshots are taken

DOI: 10.1002/fld

at the end of the period after stationary oscillations have been established. The graphs are virtually indistinguishable because the difference is very small, of order $O(10^{-8})$ for Ψ and $O(10^{-5})$ for Θ. We have found this to be the case for all $\omega \leqslant 3$ and $\varepsilon < 1$.

The results of the previous sections suffice to claim that the technique developed here is a reliable numerical instrument. This means that it can be safely applied to unravel the intricate bifurcation mechanisms that are operative in the thermoconvective flow in a vertical slot. The somewhat longer verification process has been warranted because of the fact that the proposed technique is rather new and that it will be applied in what follows to the demanding task of investigating the complex bifurcation phenomenon, which includes both isochronous and subharmonic motions.

6. STABILITY INVESTIGATION AND BIFURCATION DIAGRAMS

Now we can move to the jitter problem as outlined in the preceding. The only way to assess the results in this case is to compare with the finite-difference solution from [10]. In making this comparison we take into account the slight differences in scaling of the spatial variable x between [10] and the present study.

The criterion we used to determine whether our solution was periodically stable is actually a numerical implementation of the requirement that the Floquet exponents have real parts lesser than or equal to zero. Let $\|\Psi^{(n)}\|$ denote the quantity $|\Psi^n_{\max} - \Psi^n_{\min}|$ where the maximum and minimum are taken over one time period and the superscript n is the number of the period in question. Then, we require

$$F_{n+1} = \frac{|\|\Psi^{(n+1)}\| - \|\Psi^{(n)}\||}{\|\Psi^{(n+1)}\|} < 10^{-13} \quad \text{and that} \quad F_{n+1} - F_n < 10^{-12} \tag{37}$$

The reason for this is that for each coefficient in our spectral series we have

$$p_i^n = p_i(nT) = P_i(nT)\mathrm{e}^{\rho_i nT}$$

$$p_i^{n+1} = p_i((n+1)T) = P_i((n+1)T)\mathrm{e}^{\rho_i (n+1)T}$$

where P is a periodic function and ρ_i are the Floquet exponents.

But by the periodicity condition $P(t+T) = P(t)\ \forall t > 0$ we have $P_i((n+1)T) = P_i(nT)$, and thus

$$\frac{p_i^{n+1} - p_i^n}{p_i^{n+1}} = \frac{P_i((n+1)T)(\mathrm{e}^{\rho_i (n+1)T} - \mathrm{e}^{\rho_i nT})}{P_i((n+1)T)\mathrm{e}^{\rho_i (n+1)T}} = 1 - \mathrm{e}^{-\rho_i T} \approx \rho_i T$$

which makes (37) a valid numerical approximation of the Floquet stability criterion.

We have computed the bifurcation diagrams for two cases: the first case with $Pr = 0.73$, $Ra = 511\,650$, $\tau_B = 0.16211$ ($\gamma = 12$) (see Figure 5 of [10]), which we treat in greater detail, and the second case with $Pr = 10$, $Ra = 100\,000$, $\tau_B = 0.4$ ($\gamma = 10$). Figure 5 presents the neutral stability curves as obtained by the above presented numerical technique.

As should have been expected the minimal critical amplitudes $\varepsilon_{\min}$ are about two times smaller than [10], while the frequencies of the minimum are very slightly affected by the new scaling (differing by a couple of percentage points). This lends support for the finite-difference computations from [10].

DOI: 10.1002/fld

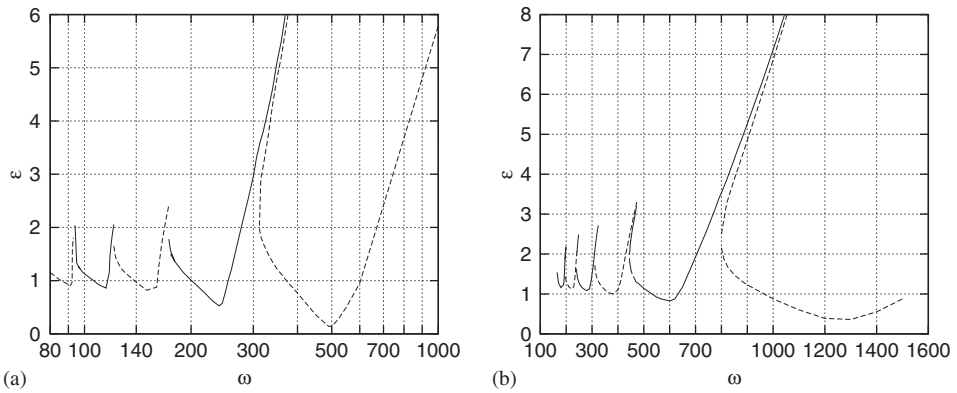

Figure 5. Bifurcation diagram. The solid-line curves present isochronous bifurcation. The dashed-line curves present a subharmonic bifurcation. (a) $Pr=0.73$, $Ra=511650$, $\tau_B=0.1611$ ($\gamma=12$); (b) $Pr=10$, $Ra=100000$, $\tau_B=0.4$ ($\gamma=10$). The alternating pattern of isochronous and subharmonic stability curves is similar to the stability diagram of the Mathieu equation.

Now, Figure 5 will help us choose some specific frequencies for which the solution still exists and can be compared. We chose to investigate two frequencies: $\omega=200$ and 500, the first belonging to the realm of isochronous bifurcation, and the second to the subharmonic bifurcation. In the first case the critical amplitude given by the finite-difference scheme is $\varepsilon_c=1.02$. In the second case we have $\varepsilon_c=0.144$.

The spatial approximation of the scheme has been thoroughly verified on the above-mentioned simple examples and due to space considerations, we do not show detailed comparisons for the profiles. However, we can trace the temporal evolution of the solution in one spatial position and to compare with the finite-difference solution. We chose $x=-0.5$ as a representative position where all variables assume nontrivial values. For comparisons we take the same number 200 of divisions of one time period in the two numerical algorithms.

6.1. Bifurcation near an isochronous branch

In order to shed light on the specific bifurcation mechanisms in operation, we choose the case $Pr=0.73$, $Ra=511650$, $\tau_B=0.16211$ ($\gamma=14$) as the featuring example.

First we begin with the case $\omega=200$. We choose a reasonably large $\varepsilon=1$, which is very close to the threshold of instability. Figure 6 presents the result. We conducted 200 time periods in order to ensure that the motion is of type of stationary oscillations and after that we calculated another 5 periods, which are actually presented in the figure. The second harmonic for both stream function and temperature is easily discernible on the figure. This is a clear demonstration of the way to isochronous bifurcation: the nonlinearity presents itself in the standard way through creating the higher harmonics. We did the same calculations for smaller $\varepsilon=0.8$ and the result has much less pronounced second mode. A much more sensitive characteristic is the critical jitter amplitude, ε_c. The truncation error has a much stronger impact on the Floquet exponents rather than on the profiles themselves. The Galerkin spectral method predicts $\varepsilon_c=1.00991$ compared with $\varepsilon_c=1.02$ of the finite-difference method. This means that the difference is less than 1.0%. Let us mention that the truncation error of the finite-difference solution with $N=320$ grid intervals is $O(1/320^2)\sim 10^{-5}$,

DOI: 10.1002/fld

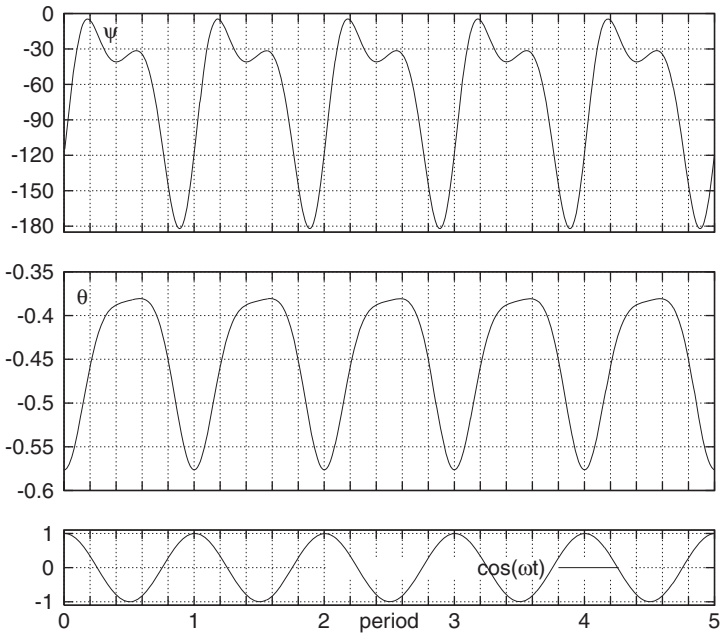

Figure 6. Typical profiles of stream function and temperature at $x=0.5$ as functions of time for the case of isochronous bifurcation at $\omega=200$ and $\varepsilon=1$ (and $Pr=0.73$, $Ra=511\,650$, $\tau_B=0.16211$, $\gamma=14$). Uppermost panel: $\Psi(-0.5,t)$; middle panel: $\Theta(-0.5,t)$; and lower panel: the forcing function $\cos(\omega t)$.

i.e. the 'phase error' of the onset of the instability is of two orders of magnitude higher. Yet both of them are small enough in this particular case. In some cases the difference increases. In such cases, the spectral method is more reliable because of the way the truncation error affects the solution in finite-difference schemes.

6.2. Bifurcation near a subharmonic-bifurcation curve

We begin with a typically subharmonic case that occurs for $\omega=500$. Here the instability first takes place for $\varepsilon=0.16$, while for $\varepsilon=0.15$ the evolution is perfectly stable. When the instability onsets at $\varepsilon=0.16$, the increase in the amplitude in time is slow but is clearly seen over the span of couple of thousands of periods. Computing the increment over a period allows us to quantify the process of divergence of the solution. The diverging oscillations have subharmonic character.

A very interesting issue here is whether the nondiverging oscillations are also subharmonic and when and how the subharmonic mode sets in. The answer is of importance for understanding the passage from 1D to 2D bifurcation. To this end we choose $\varepsilon=0.15$ and run the calculations up to 3000 time periods. Figure 7 shows four different stages of the solution for the time functions $\Psi(-0.5,t)$ and $\Theta(-0.5,t)$: after 300, 1000, 2000, and 3000 periods, respectively.

The figure shows that immediately after the beginning of the calculations, the subharmonic mode sets in. If one is not careful enough (or the algorithm used is not precise enough) one is bound to stop the calculations after the first 300 periods and to conclude that stationary oscillations of period $2T$ take place. A more careful inspection reveals that the subharmonic mode cannot

DOI: 10.1002/fld

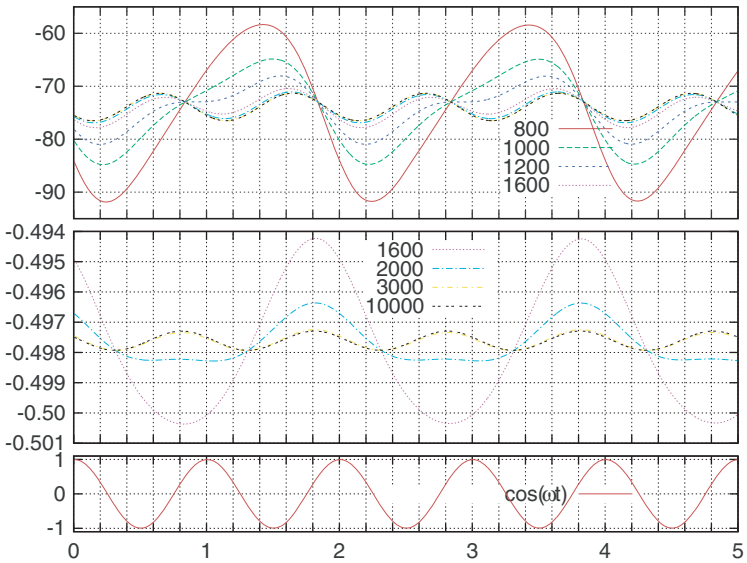

Figure 7. Profiles of the stationary oscillations after different numbers of periods for $\omega=500$, $\varepsilon=0.15$ (and $Pr=0.73$, $Ra=511650$, $\tau_B=0.16211$, $\gamma=14$). Uppermost panel: stream function; middle panel: temperature; lower panel: forcing function.

survive and profiles gradually transform into steady oscillations of isochronous type. During this transformation the amplitudes are drastically reduced so that to assume values commensurate with the small value of the loading parameter ε. The initial high amplitudes are largely due to the fact that the flow is very close to the threshold of instability. In the initial moment, the abrupt jump in the forcing function is from zero to unity driving the system temporarily out of equilibrium. Then a long transient mode sets on, which eventually returns the system to the stable isochronous oscillations.

What was said in the above applies to all values of $\varepsilon>0$, even to numerically small ones like $\varepsilon=0.001$. In all cases the initial motion after the abrupt imposition of the loading function is subharmonic. Only for smaller amplitudes, it transforms into isochronous in much shorter time—sometimes in a mere 10 periods. This result shows that the subharmonic bifurcation and doubling of the period is an innate feature of the jitter problem for some intervals of the jitter frequency ω. This calls for deeper investigation of the onset of 2D modes in the intervals of the governing parameters corresponding to the subharmonic bifurcation.

6.3. Dependence of isochronous bifurcation on jitter intensity

An important characteristic of the process is the dependence of the stream function amplitude $|\Psi|=\Psi_{\max}-\Psi_{\min}$, on the value of ε, where the maximum and minimum are taken over the last fully completed period before the stability criterion (see Section 6) is satisfied. We begin with the case of isochronous transition to instability. We demonstrate the mechanism of bifurcation for the above selected values of the governing parameters.

For values of the forcing frequency ω corresponding to isochronous bifurcations, we have found that the solution blows up in finite time. We have investigated two blow-up cases: $\omega=200$ and

DOI: 10.1002/fld

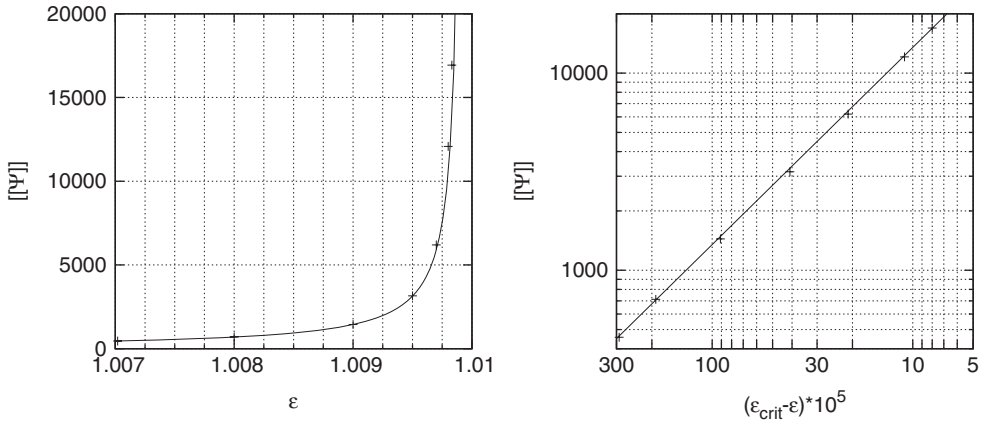

Figure 8. Dependence of stream function amplitude $|\psi|$ on the jitter amplitude for $\omega=200$. The crosses present our calculations and the solid line is the best fit curve $f(\varepsilon)=1.35/(1.00991-\varepsilon)$. Left panel: rectilinear coordinates; right panel: logarithmic coordinates in the vicinity of singularity.

250 and they are qualitatively similar. We present in Figure 8 only the case $\omega=200$ for both logarithmic and nonlogarithmic scales.

We observe that the main characteristic of the $|\Psi|$ *versus* ε graph in Figure 8, is the appearance of a singularity of the form $A(\varepsilon_c-\varepsilon)^{-\alpha}$, $\alpha>0$. This is a remarkable observation in light of the fact that the 'blow-up' in finite time is associated, as a rule, with nonlinear systems, while the linear systems diverge exponentially in infinite time, when unstable. This observation can be explained by the fact that the loading function is actually a coefficient that multiplies one of the functions (the temperature Θ in our case). In the sense of temporal evolution, the system has some of the traits of a nonlinear system, e.g. subharmonic bifurcation and 'blow-up' in a finite time. As it can be seen in the right panel of Figure 8, the fit to the data is very good, i.e. the blow-up in finite time is firmly established by our computations. This nonlinear-like response of the system under consideration is an innate feature of the problem and has been first discovered by Farooq and Homsy [9, 11] using analysis in normal modes and comparing the most dominant mode with the forcing function.

6.4. Dependence of subharmonic bifurcation on jitter intensity

The dependence $|\Psi|(\varepsilon)$ is quite different for frequencies ω that correspond to a subharmonic transition to instability. In order to elucidate this point we keep the values of Pr, Ra, and γ as in the previous subsection and choose a value for ω for which a subharmonic bifurcation takes place. We investigated the behavior for ω's belonging to three different subharmonic branches, namely $\omega=92, 170, 350$ (see Figure 5(a)). At the bifurcation point, the curve $|\Psi|(\varepsilon)$ abruptly comes to a halt because for $\varepsilon>\varepsilon_{\text{crit}}$ stationary pulsations do not exist anymore. One sees in the three panels of Figure 9 that, in this case, the amplitude $|\Psi|$ is finite for ε up to the critical value $\varepsilon_{\text{crit}}$.

There are some quantitative differences in the $|\Psi|(\varepsilon)$ dependence for the three different cases. For instance, for $\omega=170$ (shown in the middle panel of Figure 9), the slope of the amplitude increases superlinearly for smaller ε but then it exhibits an inflection point and the growth is slowed (the slope diminishes to almost zero). This can be attributed to the fact that in the case $\omega=170$

DOI: 10.1002/fld

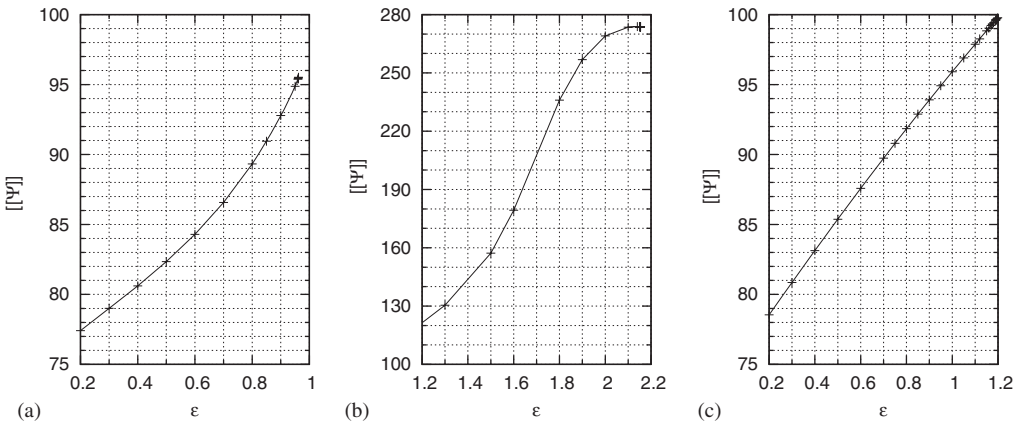

Figure 9. Dependence of stream function amplitude $[\![\psi]\!]$ on the jitter amplitude for two cases of subharmonic bifurcation. The crosses present our calculations and the solid line is the interpolating curve. (a) $\omega=92$; (b) $\omega=170$; and (c) $\omega=350$.

the critical jitter amplitude is much higher, namely $\varepsilon_{\text{crit}}\approx 2.154$. The behavior is qualitatively the same for the two frequencies $\omega=92$ and 350 for which $\varepsilon_{\text{crit}}\approx 1$.

6.5. Resonances

One can infer from the presented results that the system under consideration is absolutely stable for $\varepsilon=0$, i.e. when there is no jitter. This has been shown by Christov and Homsy [10] with the use of energy estimates. To this end, the unknown function Θ can be eliminated from Equations (5) and (6) and the following equation with constant coefficients can be derived:

$$\frac{1}{Pr}\Psi_{ttxx}=-4\gamma^4\Psi_{xx}+\left(1+\frac{1}{Pr}\right)\Psi_{txxxx}-\Psi_{xxxxxx} \tag{38}$$

Equation (38) is the same as that in [10] except for the coefficient of Ψ_{txxxx}, which reflects the different scaling here. According to [10], one may interpret (38) as a generalized wave equation with Ψ_{xxxxxx} and Ψ_{txxxx} representing dispersion and dissipation, respectively. In other words, we are faced with a slightly damped dispersive wave equation. For $Pr\sim O(1)$, these two terms are relatively small and may be disregarded. Thus, disregarding Ψ_{xxxxxx} and Ψ_{txxxx} and integrating twice with respect to x, we obtain

$$\Psi_{tt}=-4\gamma^4 Pr\,\Psi$$

This is the equation of a simple harmonic oscillator with cyclic frequency

$$\omega_r=2\gamma^2 Pr^{1/2} \tag{39}$$

Substituting $Pr=0.73$, $Ra=511650$, $\tau_B=0.16211$ ($\gamma=12$) into Equation (39) we obtain that $\omega_r=246.067$. One sees that this specific value of ω_r corresponds to a minimum of the bifurcation curve in Figure 5(a). The number $2\omega_r$ also corresponds roughly to another minimum of the curve, which leads to the conclusion that we observe a behavior similar to the Mathieu equation

DOI: 10.1002/fld

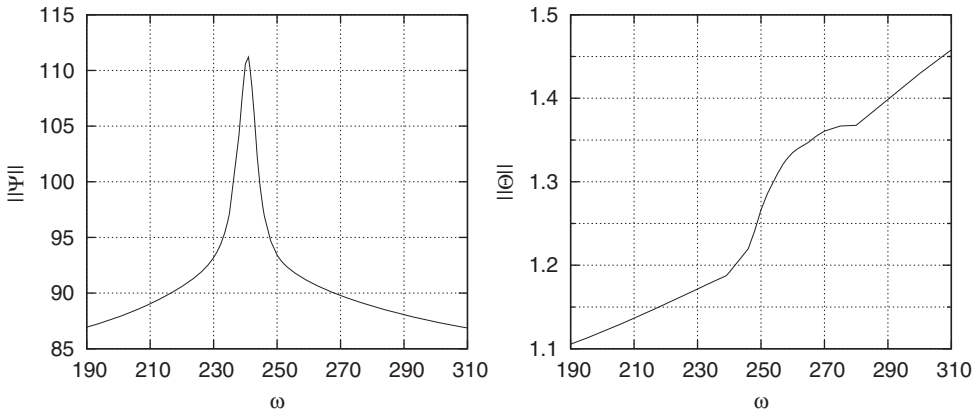

Figure 10. The behavior of the response amplitudes $\|\Psi\|$, $\|\Theta\|$ as functions of ω for $\varepsilon=0.5$.

(see [18]) with strong resonant interactions between the natural modes of the system and the forcing term.

If there were no damping, the curves in Figure 5 should go down to zero at the resonance frequencies (see the respective graph for the Mathieu equation). Hence, the minima in our curves qualitatively represent the quasi-frequencies of 'resonance' of the damped oscillator under study. Note, though, that it is not only the Prandtl number that may cause a departure from the expected resonance frequency but also the fact that, in reality, the coefficient $-4\gamma^4[1+\varepsilon\cos(\omega t)]$ of the term Ψ_{xx} in (38) depends on time.

The assertion that resonances occur when the G-jitter interacts with the natural convective modes is further corroborated by our investigation of the response amplitude behavior as a function of gravity modulation frequency ω. We varied ω, keeping all other parameters fixed: $Pr=0.73$, $\varepsilon=0.5$, $Ra=511650$, $\tau_B=0.16211$. The result is presented in Figure 10.

The stream function shows a typical resonance pattern with its amplitude $|\Psi|(\omega)$ peaking near the above computed value $\omega_r=246.067$. The slope of the temperature field exhibits a significant increase in the vicinity of ω_r, which means that the derivative of the $|\Theta|(\omega)$ exhibits a spike similar to the one for the stream function.

7. CONCLUSIONS

In the present study a Galerkin technique is developed for coupled thermoconvective flows in a vertical slot. A specialized spectral numerical technique is developed for solving the problem. The well-known beam functions that satisfy four boundary conditions are used as the basis set for the stream function together with the trigonometric functions for the temperature. The formulas for the cross-expansion of the two systems were not available in the literature and are derived here alongside with various miscellaneous expressions needed for the successful implementation of the Galerkin technique.

The developed numerical technique is applied to the 1D unsteady problem of thermoconvection in a vertical slot with both horizontal and vertical gradients of the temperature. This is a higher order in space initial-boundary value problem with multi-dimensional parametric space, which can

DOI: 10.1002/fld

be interrogated successfully only if the algorithm is fast enough. The developed here algorithm presents such a highly accurate and efficient technique. The performance of the numerical algorithm is validated for various limiting cases when exact or approximate analytical solutions are available.

By means of the developed here algorithm, we gained an insight into the physical nature of the bifurcation and the parametric instability. There were some suggestions in the literature that for the problem under consideration there exist two kinds of parametric instability: isochronous and subharmonic. Here we have found that the stable motions of type of stationary oscillations are always isochronous, while the unstable motions can be either isochronous or subharmonic. Another novel conclusion from the numerical experiments of the present study is that in the intervals for the frequency ω where the instability is in the subharmonic mode, the evolution of the solution *always* does start from a subharmonic shape. Then in the stable cases a transient regime takes place, which transforms the motion from subharmonic to isochronous mode. The duration of this transient increases drastically near the threshold of instability. For amplitudes very close to the critical one, the transient may span several thousands of time periods before the solution settles back to the isochronous shape.

The dependence of the amplitude of the solutions on some of the parameters has also been investigated. We have found that for ω corresponding to isochronous bifurcation we have a singular dependence of the form $\|\Psi\| \sim 1/(\varepsilon_{\text{crit}} - \varepsilon)$, whereas there is no singularity for ω corresponding to subharmonic bifurcations. In other words, for the isochronous cases the solution 'blows up' in finite time, which makes this apparently linear system akin to some nonlinear systems. We have also shown that resonances occur when the forcing frequency approaches the natural frequency of the convective modes.

Thus, a new instrument for numerical investigation of thermoconvective modulated flows has been created and new physical results have been obtained.

APPENDIX A: EXISTENCE AND COMPLETENESS OF BEAM FUNCTIONS

Theorem A.1
The eigenfunctions of (7) as given by (8), (9) form a CON set of functions on $C^4[-1, 1]$.

Proof (*Sketch*)
We follow the method of Coddington and Levinson (see [19]) for nth order self-adjoint problems. First, we prove the existence of the eigenfunctions. Let $\mathscr{G}$ be the operator defined by

$$\mathscr{G} f(x) = \int_{-1}^{1} G(x, \tau) f(\tau)\, \mathrm{d}\tau \tag{A1}$$

where f is any continuous function on $[-1, 1]$ and $G(x, \tau)$ is Green's function[‡] corresponding to (7). Here,

$$G(x, \tau) = \begin{cases} -\frac{1}{24}(x-1)2(1+\tau)2(-1+x(\tau-2)+2\tau), & \tau \leqslant x \\ -\frac{1}{24}(x+1)2(\tau-1)2\,(-1-2x+x(\tau+2)), & \tau > x \end{cases} \tag{A2}$$

[‡]For more details on the derivation of $G(x, \tau)$ and the properties it satisfies see [17, 19].

DOI: 10.1002/fld

The operator $\mathscr{G}$ can be understood as an inverse operator to $\mathscr{L} \equiv \mathrm{d}4/\mathrm{d}x$ in the sense that

$$\mathscr{L}\mathscr{G} f = f, \quad \mathscr{G}\mathscr{L} u = u \tag{A3}$$

are valid for all $f \in C[-1, 1]$ and $u \in C^4[-1, 1]$ which satisfy the boundary conditions. The eigenfunctions of $\mathscr{G}$ are the same as the eigenfunctions of (7), and the eigenvalues of $\mathscr{G}$ are the inverses of the eigenvalues of (7). Hence, it is sufficient to show the existence result for $\mathscr{G}$. This is done by showing that $\|\mathscr{G}\| = \sup_{\|u\|=1} \|\mathscr{G}u\|$ is the maximal eigenvalue of $\mathscr{G}$. The remaining eigenvalues and corresponding eigenfunctions of $\mathscr{G}$ are then constructed and it is shown that there is an infinite number of monotonically decreasing eigenvalues.

Finally, to demonstrate the completeness, the monotonicity of the eigenvalues and Bessel's inequality are applied to show that the Fourier–Galerkin expansion

$$f = \sum_{k=0}^{\infty} \langle f, \chi_k \rangle \chi_k \tag{A4}$$

of f into eigenfunctions of (7) converges uniformly to f on $[-1, 1]$. □

APPENDIX B: PRODUCTS OF BEAM FUNCTIONS

Product formulas are essential for the application of our technique to nonlinear problems.The expressions for developing the nonlinear terms into series with respect to the system appeared simultaneously in [4, 20] though in a different form. We stick here to the notations of [4] as more explicit and easier to verify:

$$\begin{aligned} c_n(x)c_m(x) = \sum_{k=1}^{\infty} h_k^{nm} c_k(x), \quad \sqrt{2}h_k^{nm} = \sqrt{2}\int_{-1}^{1} c_n(x)c_m(x)c_k(x)\,\mathrm{d}x \\ = \frac{-(\kappa_m+\kappa_k)(\tanh\kappa_m+\tanh\kappa_k)-\kappa_n\tanh\kappa_n}{(\kappa_m+\kappa_k)^2-\kappa_n^2} \\ + \frac{-(\kappa_m-\kappa_k)(\tanh\kappa_m-\tanh\kappa_k)+\kappa_n\tanh\kappa_n}{-(\kappa_m-\kappa_k)^2+\kappa_n^2} \\ + \frac{-(\kappa_m+\kappa_k)(\tanh\kappa_m+\tanh\kappa_k)+\kappa_n\tanh\kappa_n}{(\kappa_m+\kappa_k)^2+\kappa_n^2} \\ + \frac{-(\kappa_m-\kappa_k)(\tanh\kappa_m-\tanh\kappa_k)+\kappa_n\tanh\kappa_n}{(\kappa_m-\kappa_k)^2+\kappa_n^2} \\ + \frac{-(\kappa_n+\kappa_k)(\tanh\kappa_n+\tanh\kappa_k)+\kappa_m\tanh\kappa_m}{(\kappa_n+\kappa_k)^2+\kappa_m^2} \\ + \frac{-(\kappa_n-\kappa_k)(\tanh\kappa_n-\tanh\kappa_k)+\kappa_m\tanh\kappa_m}{(\kappa_n-\kappa_k)^2+\kappa_m^2} \\ + \frac{-(\kappa_n+\kappa_m)(\tanh\kappa_n+\tanh\kappa_m)+\kappa_k\tanh\kappa_k}{(\kappa_n+\kappa_m)^2+\kappa_k^2} \\ + \frac{-(\kappa_n-\kappa_m)(\tanh\kappa_n-\tanh\kappa_m)+\kappa_k\tanh\kappa_k}{(\kappa_n-\kappa_m)^2+\kappa_m^2} \end{aligned} \tag{B1}$$

DOI: 10.1002/fld

$$s_n c_m = \sum_{k=1}^{\infty} f_k^{nm} s_k, \quad s_n s_m = \sum_{k=1}^{\infty} f_m^{nk} c_k, \quad \sqrt{2} f_k^{nm} = \sqrt{2} \int_{-1}^{1} s_n c_m s_k \, \mathrm{d}x$$

$$\begin{aligned}
&= \frac{(\lambda_n + \lambda_k)(\coth \lambda_n + \coth \lambda_k) - \kappa_m \tanh \kappa_m}{(\lambda_k + \lambda_n)^2 - \kappa_m^2} \\
&+ \frac{-(\lambda_k - \lambda_n)(\coth \lambda_k - \coth \lambda_n) + \kappa_m \tanh \kappa_m}{(\lambda_k - \lambda_n)^2 - \kappa_m^2} \\
&+ \frac{-(\lambda_k + \kappa_m)(\coth \lambda_k + \tanh \kappa_m) + \lambda_n \coth \lambda_n}{(\lambda_k + \kappa_m)^2 + \lambda_n^2} \\
&+ \frac{-(\lambda_k - \kappa_m)(\coth \lambda_k - \tanh \kappa_m) + \lambda_n \coth \lambda_n}{(\lambda_k - \kappa_m)^2 + \lambda_n^2} \\
&+ \frac{-(\lambda_n + \kappa_m)(\coth \lambda_n + \tanh \kappa_m) + \lambda_k \coth \lambda_k}{(\lambda_n + \kappa_m)^2 + \lambda_k^2} \\
&+ \frac{-(\lambda_n - \kappa_m)(\coth \lambda_n - \tanh \kappa_m) + \lambda_k \coth \lambda_k}{(\lambda_n - \kappa_m)^2 + \lambda_k^2} \\
&+ \frac{-(\lambda_n + \lambda_k)(\coth \lambda_n + \coth \lambda_k) + \kappa_m \tanh \kappa_m}{(\lambda_k + \lambda_n)2 + \kappa_m^2} \\
&+ \frac{(\lambda_k - \lambda_n)(\coth \lambda_n - \coth \lambda_k) + \kappa_m \tanh \kappa_m}{(\lambda_k - \lambda_n)^2 + \kappa_m^2}
\end{aligned} \tag{B2}$$

These formulas were thoroughly tested in [14].

REFERENCES

1. Boyd JP. *Fourier and Chebyshev Spectral Methods*. Dover: New York, 2000.
2. Rayleigh L. *Theory of Sound*. Dover: New York, 1945.
3. Poots G. Heat transfer by laminar free convection in enclosed plane gas layers. *Quarterly Journal of Mechanics and Applied Mathematics* 1958; **11**:357–273.
4. Christov CI. A method for treating the stochastic bifurcation of plane Poiseuille flow. *Annuaire de l'Université dè Sofia "Kliment Ohridski", Faculté de Mathématiques et Mechanique* 1982; **76**(lb.2-Mecanique):87–113.
5. Papanicolaou N, Christov CI. Galerkin spectral method for higher-order boundary value problems arising in thermal convection. *Annuaire de l'Université dè Sofia* 2000; **94**:71–83.
6. Christov CI, Papanicolaou N. Galerkin spectral methods for higher-order boundary-value problems arising in fluid mechanics. *Proceedings of the Thirtieth Spring Conference of the Union of Bulgarian Mathematicians*, Borovets, 8–11 April 2001; 438–443.
7. Papanicolaou NC, Christov CI. A Galerkin spectral method for thermoconvection boundary value problems. *Journal of Neural Parallel and Scientific Computations* 2002; **10**(3):339–354.
8. Bergholz RF. Instability of steady natural convection in a vertical fluid layer. *Journal of Fluid Mechanics* 1978; **84**:743–768.
9. Farooq A, Homsy GM. Linear and nonlinear dynamics of a differentially heated slot under gravity modulation. *Journal of Fluid Mechanics* 1996; **313**:1–38.
10. Christov CI, Homsy GM. Nonlinear dynamics of two dimensional convection in a vertically stratified slot with and without gravity modulation. *Journal of Fluid Mechanics* 2001; **430**:335–360.

DOI: 10.1002/fld

11. Farooq A, Homsy GM. Streaming flows due to g-jitter-induced natural convection. *Journal of Fluid Mechanics* 1994; **271**:351–378.
12. Suresh VA, Christov CI, Homsy GM. Resonant thermocapillary and buoyant flows with finite frequency gravity modulation. *Physics of Fluids* 1999; **11**:2565–2576.
13. Chandrasekhar S. *Hydrodynamic and Hydromagnetic Instability*. Oxford University Press: Clarendon, London, 1961.
14. Papanicolaou NC, Christov CI. On the beam-functions spectral expansions for fourth-order boundary value problems: advantages and disadvantages. *Thirty-third International Conference on Applications of Mathematics in Engineering and Economics*, *American Institute of Physics CP 946*, Sozopol, Bulgaria, 8–14 June 2007. Springer: Berlin, 2007; 119–126.
15. Harris DL, Reid WH. On orthogonal functions which satisfy four boundary conditions. I. Tables to use in Fourier-type expansions. *Abstract of Astrophysical Journal*, *Supplement Series* 1958; **III**(33):429–447.
16. Reid WL, Harris DL. On orthogonal functions which satisfy four boundary conditions. II. Integrals to use in Fourier-type expansions. *Abstract of Astrophysical Journal*, *Supplement Series* 1958; **III**(33):448–452.
17. Papanicolaou NC. A Galerkin spectral method for fourth-order boundary value problems. *Ph.D. Thesis*, University of Louisiana at Lafayette, 2003.
18. Jordan DW, Smith P. *Nonlinear Ordinary Differential Equations*: *An Introduction to Dynamical Systems*. Oxford University Press: Oxford, U.K., 1999.
19. Coddington EA, Levinson N. *Theory of Ordinary Differential Equations*. McGraw-Hill: New York, 1955.
20. Jhaveri BS, Rosenberger F. Exact triple integrals of beam functions. *Journal of Computational Physics* 1982; **45**:300–302.

DOI: 10.1002/fld